Illuminating Phenylazopyridines To Photoswitch Metabotropic Glutamate Receptors: From the Flask to the Animals

Xavier Gómez-Santacana, Silvia Pittolo, Xavier Rovira, Marc Lopez, Charleine Zussy, James Dalton, Adèle Faucherre, Chris Jopling, Jean-Philippe Pin, Francisco Ciruela, et al.

ACS central science

Research Article

http://pubs.acs.org/journal/acscii

Illuminating Phenylazopyridines To Photoswitch Metabotropic Glutamate Receptors: From the Flask to the Animals

Xavier Gómez-Santacana,[†,‡,§,∥] Silvia Pittolo,[‡] Xavier Rovira,[⊥,#] Marc Lopez,[¶,Ψ] Charleine Zussy,[⊥,#] James A. R. Dalton,[§] Adèle Faucherre,[⊥,#] Chris Jopling,[⊥,#] Jean-Philippe Pin,[⊥,#] Francisco Ciruela,[¶,Ψ] Cyril Goudet,[⊥,#] Jesús Giraldo,[§,√] Pau Gorostiza,[*,‡,ɤ,∞] and Amadeu Llebaria[*,†]

[†]MCS, Laboratory of Medicinal Chemistry & Synthesis, Institute for Advanced Chemistry of Catalonia (IQAC−CSIC), Barcelona, Spain

[‡]Institute for Bioengineering of Catalonia (IBEC), Barcelona, Spain

[§]Institut de Neurociències and Unitat de Bioestadística, Universitat Autònoma de Barcelona (UAB), Barcelona, Spain

[⊥]Institute of Functional Genomics, Université de Montpellier, Unité Mixte de Recherche 5302 CNRS, Montpellier, France

[#]Unité de recherche U1191, INSERM, Montpellier, France

[¶]Unitat de Farmacologia, Departament Patologia i Terapèutica Experimental, Facultat de Medicina, IDIBELL, Universitat de Barcelona, Barcelona, Spain

[Ψ]Institut de Neurociències, Universitat de Barcelona, Barcelona, Spain

[√]Network Biomedical Research Center on Mental Health (CIBERSAM), Madrid, Spain

[ɤ]Network Biomedical Research Center on Bioengineering, Biomaterials and Nanomedicine (CIBER-BBN), Madrid, Spain

[∞]Catalan Institution for Research and Advanced Studies (ICREA), Barcelona, Spain

Supporting Information

ABSTRACT: Phenylazopyridines are photoisomerizable compounds with high potential to control biological functions with light. We have obtained a series of phenylazopyridines with light dependent activity as negative allosteric modulators (NAM) of metabotropic glutamate receptor subtype 5 ($mGlu_5$). Here we describe the factors needed to achieve an operational molecular photoisomerization and its effective translation into *in vitro* and *in vivo* receptor photoswitching, which includes zebrafish larva motility and the regulation of the antinociceptive effects in mice. The combination of light and some specific phenylazopyridine ligands displays atypical pharmacological profiles, including light-dependent receptor overactivation, which can be observed both *in vitro* and *in vivo*. Remarkably, the localized administration of light and a photoswitchable compound in the peripheral tissues of rodents or in the brain amygdalae results in an illumination-dependent analgesic effect. The results reveal a robust translation of the phenylazopyridine photoisomerization to a precise photoregulation of biological activity.

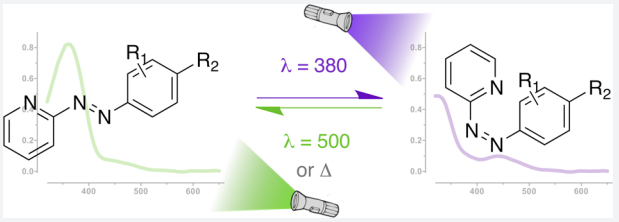

INTRODUCTION

The therapeutic use of chemical compounds has historically driven medicine to exceptional achievements in the prevention and treatment of diseases.[1] Drug discovery is now a multidisciplinary activity in permanent motion to achieve new therapeutic challenges for unmet clinical needs. However, in spite of increasing R&D efforts, continuous technical progress, and outstanding scientific achievements, new drugs are scarce.[2] Although the reasons for this are multiple, drug discovery is facing problems associated with the increasing complexity of diseases and therapeutic targets, which require more precise therapeutics and can be connected to the lack of effective and truly innovative medicines.[3] Conventional pharmacology involves drug interaction with a target protein and the induction of changes in its functional activity to trigger the therapeutic response. However, in practice after the drug is systemically administered to an organism, the precise control of its action at the target protein is lost.[4] Photopharmacology may provide solutions to this problem since it enables the spatiotemporal control of target proteins with light-regulated receptor-specific drugs.[5,6] In particular, light can restrain the drug action site and enable accurate dosing patterns[5] that can be adjusted in real-time mode.

Photopharmacological strategies have proven successful in the regulation of free ligands of ion channels[4,6] and inhibitors of protein−protein interactions[7] but in many cases require genetic modification of the target receptor.[8] Genetic manipulation can

Received: November 15, 2016
Published: December 19, 2016

DOI: 10.1021/acscentsci.6b00353
ACS Cent. Sci. 2017, 3, 81−91

be circumvented by drug azologization,[9−11] which is based on the insertion of azobenzene units into the chemical scaffold of existing ligands to obtain new photoswitchable molecules but maintaining the drug-like properties of the original ligand.[9,10] Some successful examples are bis-Q,[12] gluazo,[13] azo-propofols,[14] AzoTHA,[15] fotocaine,[9] JB253,[16] and PST-1.[17]

Recently, we reported on alloswitch-1 (**1a**)[11] (Figure 1A), a phenylazopyridine derivative as the first GPCR photoswitchable allosteric modulator with activity *in vivo*.

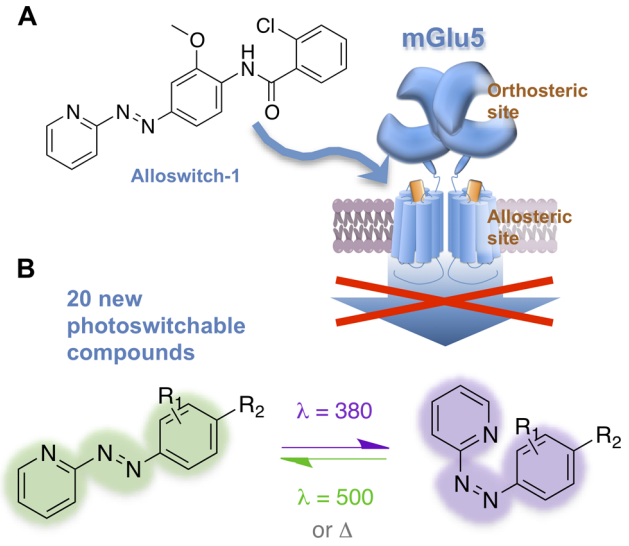

Figure 1. Design of the phenylazopyridine series. (A) Alloswitch-1 is a photoswitchable allosteric inverse agonist of $mGlu_5$, in its *trans* configuration. (B) We designed and synthesized 20 photoswitchable derivatives of alloswitch-1, with the same phenylazopyridine scaffold. With violet light (380 nm) they switch from the thermodynamically stable *trans* isomer to the *cis* isomer and switch back to the *trans* isomer with green light (500 nm) or thermally, without illumination.

Instead of the classical photoisomerizable azobenzene, we used a structurally related phenylazopyridine, which includes several potential advantages such as a better solubility and a faster thermal decay of the *cis* to the *trans* isomer enabling a potentially better spatiotemporal control of the activity of the compound. There are some drugs containing a phenylazopyridine scaffold, with different biological activities,[18−24] but they have not been described or exploited as photoswitchable entities or light-dependent drugs. In contrast, alloswitch-1 selectively exhibited a potent negative allosteric modulation (NAM) activity of $mGlu_5$ receptor, which belongs to the metabotropic glutamate (mGlu) GPCR family and controls important neuronal and glial functions.[25] Indeed, the *trans* isomer of alloswitch-1 inhibited $mGlu_5$ agonist response at nanomolar concentrations, whereas it was inactive in the *cis* configuration. Another phenylazopyridine (SIB-1757)[26] was previously reported as an $mGlu_5$ NAM with an IC_{50} in the nanomolar range, but its photoswitching properties were never studied. Two other potent $mGlu_5$ NAMs, MPEP and XGS-RC-009, maintain a high structural resemblance to SIB-1757 and alloswitch-1, but they include a phenylethynylpyridine moiety instead of the phenylazopyridine[27] (Chart 1), maintaining similar $mGlu_5$ NAM activity. Taking advantage from this structural parallelism and as many potent $mGlu_5$ NAMs preserve the 2-arylethynylpyridine structure, such as MPEP, GRN-529, STX107, and Raseglurant[28] (Chart 1), we designed a family of potent $mGlu_5$ NAMs based on the 2-phenylazopyridine scaffold. With these compounds we intended to determine the molecular and photochemical features that define an efficient photoreversible ligand for operating in cells and living animals. We also investigated whether these molecules can be used to effectively control temporal dosing patterns with light in biological systems.

Interestingly, while exploring the photoswitching properties of these phenylazopyridines, we found that some compounds induced an overactivation of the receptor activity *in vitro* and increased animal motility *in vivo*. We also report on these light-dependent atypical pharmacological profiles.

Chart 1. $mGlu_5$ NAMs with 2-Arylethynylpyridine, SIB-1757, and Fenobam

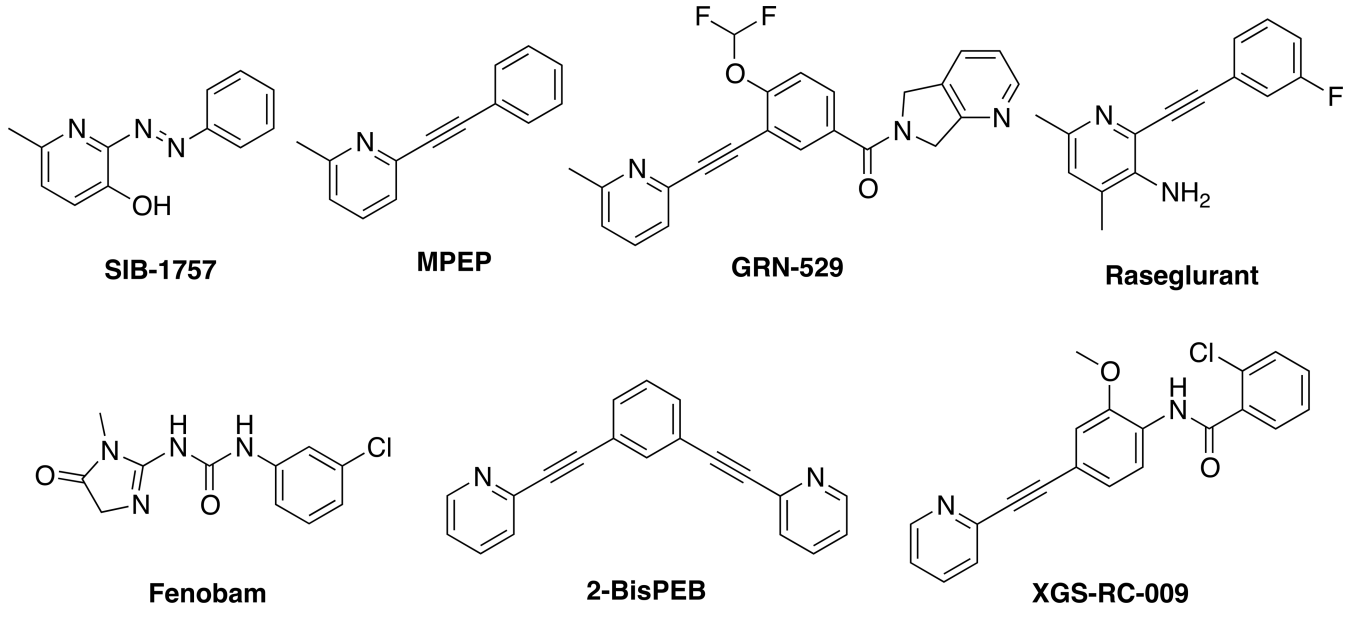

DOI: 10.1021/acscentsci.6b00353
ACS Cent. Sci. 2017, 3, 81−91

Table 1. Structure–Activity Relationship and Photoswitching Properties of the Phenylazopyridine Series[a]

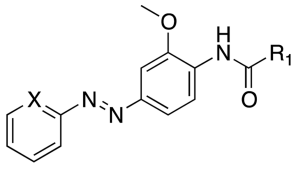

1 X = N
2 X = CH

Comp.	R_1	Max abs /nm	illum λ /nm	PIS		$t_{1/2}$ / s	Dark IC_{50} ± SEM/nM	PPS
1a	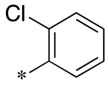	374	380	5	3	54	297±77	5.1
1b	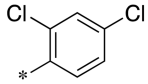	372	380	4	3	25	904±82	7.1
1c	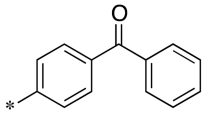	380	380	3	2	19	1884±44	1.7
1d		374	380	4	4	489	183±36	3.7
1e		374	380	4	3	556	30±4	3.7
1f		377	380	5	3	353	76±12	4.8
1g		377	380	4	3	71	180±28	4.1
1h		375	380	3	2	65	308±43	4.1
1i		377	380	4	3	41	328±18	2.5
1j		382	380	4	4	134	309±5	2.9
1k		373	380	1	1	15	356±57	1.3
1l	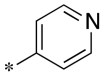	372	380	1	0	13	1025±257	1.2
2	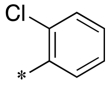	366	380	5	4	187	4667±392*	2.5

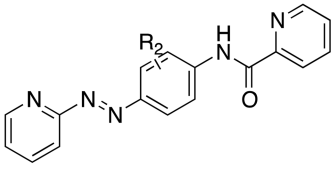

Comp.	R	Max abs /nm	illum λ /nm	PIS*		$t_{1/2}$ / s	Dark IC_{50} ± SEM/nM	PPS*
1j	3-OMe	382	380	4	4	134	309±5	2.9
3a	2-OMe	385	380	5	4	75	31661±3601	n.m.
3b	3-CN	348	380	4	0	25	2002±334	3.6
3c	H	358	380	5	4	322	3209±269	n.m.

DOI: 10.1021/acscentsci.6b00353
ACS Cent. Sci. 2017, 3, 81–91

Table 1. continued

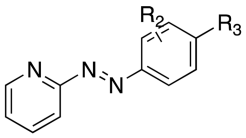

Comp.	R_2	R_3	Max abs /nm	illum λ /nm	PIS		$t_{1/2}$ / s	Dark IC_{50} ± SEM/nM	PPS
4	3-OMe	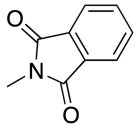	319	380	3	2	245	2496±32	3.2
5	3-OMe	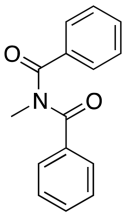	329	380	3	2	46	1477±265	3.3
6	3-OMe	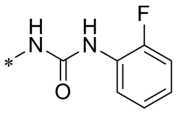	387	380	2	1	10	1204±220	4.4
				400	5	4	10	2184±663	12.3
7	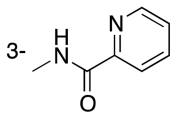	H	309	380	2	1	62	14029±1826	1.5
8	H	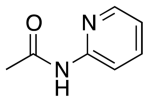	326	380	1	0	-	7785±640	2.1
9	H	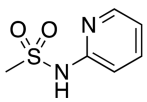	323	380	1	0	-	n.a.	

[a]PIS corresponds to photoisomerization score, $t_{1/2}$ corresponds to the *cis* isomer thermal half-life, and PPS corresponds to photoinduced potency shift (see text).

RESULTS AND DISCUSSION

Initial Considerations. In the effort of designing pharmacologically useful compounds for receptor activity photoswitching, we considered three necessary conditions: (a) biocompatible wavelengths of illumination for photoswitching, preferably in the visible range; (b) a significant difference on the relative populations of the isomers between the dark and illuminated conditions, which can be afforded with a suitable thermal relaxation of the *cis* isomer; and (c) a large difference in affinity/functional activity on the target protein between the *trans* and *cis* photoisomers.

Alloswitch-1 (**1a**) reasonably fulfilled these conditions and allowed us to control $mGlu_5$ activity with light and to induce light-dependent activity in behavioral experiments with living animals, as detailed in our previous communication.[11] In contrast, SIB-1757,[26] a potent phenylazopyridine $mGlu_5$ NAM, showed neither photoisomerization in solution nor light-induced receptor activity switch despite the structural analogy with alloswitch-1 in our hands (Supporting Information). This lack of detection of photoisomerization may be due to an azo−hydrazone tautomeric equilibrium induced by the hydroxyl of SIB-1757, which prompts a fast thermal relaxation of its *cis* isomers on the order of milliseconds[29] and suggests that not all the azobenzene ligands are well suited for controlling protein activity with light. In addition, strong electron-donating substituents in phenylazopyridines induce a push−pull effect, since the pyridine acts as an electron-withdrawing group, and this leads to a further decrease of the *cis* isomer lifetime,[30] especially in polar solvents.[31] Overall, these results confirmed that the identification of an azocompound with a suitable pharmacological activity profile is a necessary but not sufficient condition to define a useful photoswitchable ligand.

Therefore, to design compounds for $mGlu_5$ allosteric photoregulation, we maintained the amide bond present in alloswitch-1 for most of the compounds of the series and we explored the structural determinants for reaching effective receptor control with light, by changing the carboxamide substituents (Table 1). Thus, we synthesized (Supporting Information) more bulky derivatives (**1b,c**) and others with aliphatic amide substituents (**1d−f**), less bulky aromatic carboxamides (**1g,h**), or heterocyclic rings (**1i,l**) (Table 1).

To investigate the effect of the pyridine ring in alloswitch-1 (**1a**), we replaced it by a phenyl (**2**). We were also interested in the effects of the substitution in the central ring; therefore we changed the position of the methoxy group (**3a**) or replaced it by cyano (**3b**) or hydrogen (**3c**) substitutions.

Finally, we explored some changes on the amide group functionality, obtaining the imides **4** or **5** or the urea **6**. We also

DOI: 10.1021/acscentsci.6b00353
ACS Cent. Sci. 2017, 3, 81−91

explored the positional isomers **7** and **8** and also synthesized the sulfonamide **9**. All these groups were expected to confer different electronic and structural properties to the phenylazopyridine moiety, thereby altering their photoisomerization response.

UV−Vis Absorption Spectra. We measured the UV−vis absorption spectra of the *cis* and *trans* phenylazopyridine isomers after chromatographic separation with HPLC-PDA-MS (Supporting Information). The *trans* isomers presented typical light absorption for the $\pi-\pi^*$ band, in the range between 310 and 400 nm, even though for most of the phenylazopyridine compounds the maximum of this band was found around 380 nm (Figure 2A). The azobenzene *cis* isomers displayed a typical $n-\pi^*$ band with maxima in the range 420−450 nm (Figure 2B)

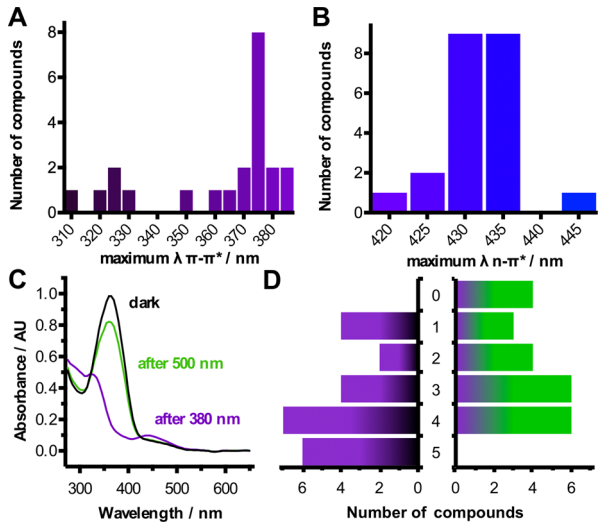

Figure 2. Spectroscopic and photosiomerization properties. (A, B) Distribution of wavelengths of absorption in the UV−vis spectrum of compounds in the series, detected by HPLC-PDA-MS (see Supporting Information). Maximum of the band corresponding to (A) $\pi-\pi^*$ transition for the *trans* isomers and (B) $n-\pi^*$ transition for the *cis* isomers. (C) Example of UV−vis absorption spectra corresponding to compound **3c**, 25 μM in DMSO. The black line corresponds to the initial spectrum in dark conditions, the violet line to the spectrum after illumination at 380 nm, and the green line after illumination at 500 nm. Comparison of these curves with the spectra of pure *trans* and *cis* isomers, obtained from HPLC-PDA-MS analysis (see Supporting Information), results in a full conversion from *trans* to *cis* isomer and near complete back-isomeration from *cis* to *trans* isomer. (D) Distribution of photoisomerization scores (PIS) for phenylazopyridines under illumination at 380 nm (violet bars) and at 500 nm (green bars) (see text and Supporting Information).

The wavelength of the maximum of these bands fundamentally depends on the nature of the substituents on the aromatic rings of the azocompound,[32] in particular electron-donating substituents in *ortho* or *para* position.[32] However, in our cases, the 2-pyridyl group, which is a π-electron-deficient heterocycle, induces a certain push−pull character to the azobenzene, especially in polar solvents.[29] Then, to achieve a proper $\pi-\pi^*$ band suitable for our interests, mild electron-donating substituents are needed to shift the maximum to longer wavelengths. An example of such is the high electron-withdrawing sulfonamide of compound **9** shifting the band to energetically higher wavelengths (310 nm), which are not suitable for biological experiments. On the other hand, the urea from compound **6**, having a more electron-donating character than the amides, shifts the band to the visible range of the spectrum (387 nm). Moreover, we found a noticeable correlation between this shift in the $\pi-\pi^*$ band and the electron density of the azo moiety (Supporting Information).

Photoisomerization Studies. To measure the extent of photoisomerization, we measured the UV−vis absorption spectra of all compounds in the dark, after illumination with violet light (λ = 380 nm) and after illumination with green light (λ = 500 nm) under light conditions similar to those used in pharmacological experiments (Figure 2C, Supporting Information). In the dark, we practically detected only the *trans* isomer. We selected 380 nm illumination (violet) to induce the *trans* to *cis* isomerization, according to the position of the *trans* isomer $\pi-\pi^*$ bands and the *cis* isomer $\pi-\pi^*$ and $n-\pi^*$ (Supporting Information). After that, we used green light (λ = 500 nm) to accelerate the opposite isomerization to the thermodynamically stable *trans* isomer.

With the information obtained from these spectra we calculated a "photoisomerization score" (PIS), to account for the effectiveness of the photoswitch and compare the molecules (5, efficient switching; 0, poor switching, see Supporting Information). A large part of the compounds of the series have photoisomerization efficiency similar to or better than that of alloswitch-1 (**1a**) (Table 1, Figure 2D). However, in some cases, compounds with a similar structure, such as pyridylamides **1k** and **1l**, have a very poor photoswitching behavior, possibly due to the fast thermal decay from the *cis* to the *trans* isomer (Table 1, Supporting Information). Moreover, we found a trend correlation in between the photoswitching effectiveness and the thermal relaxation rate (Supporting Information).

Additionally, the efficacy of the observed photoisomerization also depends on the selection of a suitable wavelength. For example, some compounds such as **2** or **3c**, despite having the maximum of absorption at 366 and 358 nm respectively, display the maximal absorbance difference between the *cis* and *trans* isomers around 380 nm (375 and 370 nm, respectively). This indicates that the optimal wavelength for illumination does not necessarily correspond to that of maximum absorption, but to the wavelength that maximizes the difference of absorption between the *trans* and the *cis* isomers (Figure 2C). An illustrative example is the urea **6**, which has its $\pi-\pi^*$ band maximum at 387 nm and a maximal *cis*−*trans* absorbance difference at 395 nm. This compound has a PIS of 2 when illuminated at 380 nm, but PIS reaches up to 5 at 400 nm achieving a practically complete isomerization, despite the fast relaxation of the *cis* isomer ($t_{1/2}$ = 10 s).

In summary, we have shown that compounds like alloswitch-1, **1f**, **2**, **3a**, **3c**, or **6** have photoisomerization properties that make them suitable potential candidates for $mGlu_5$ photoswitching applications. However, other compounds like **7**, **8**, or **9** require harmful short UV wavelengths to achieve a proper photoisomerization whereas some others such as **1k**, **1l**, or SIB-1757 have too fast *cis*−*trans* relaxation rates that limit their practical use in biological applications.

Pharmacological Activity on $mGlu_5$ Receptor in Cell-Based Assays. To study the activity of the phenylazopyridines, we generated dose−response curves of the complete series (IP accumulation assay with HEK293 expressing $mGlu_5$ receptor) to quantitatively evaluate the antagonistic activity of the series to quisqualate. We excluded compound **9**, which was found inactive in an initial screening (Supporting Information). To evaluate the light-dependent effects, we simultaneously generated two curves for each compound, by incubating the

DOI: 10.1021/acscentsci.6b00353
ACS Cent. Sci. 2017, 3, 81−91

cells with the azocompounds in the dark and under illumination at 380 nm (Supporting Information). As a result, we obtained the potencies (IC_{50}) for each compound under both conditions. Exceptionally, compound **6** was also tested under illumination at 400 nm.

In the dark, the phenylazopyridines displayed IC_{50}s in the range from low nanomolar to micromolar (Table 1 and Figure 3A). The aliphatic carboxamides **1e** and **1f** displayed low

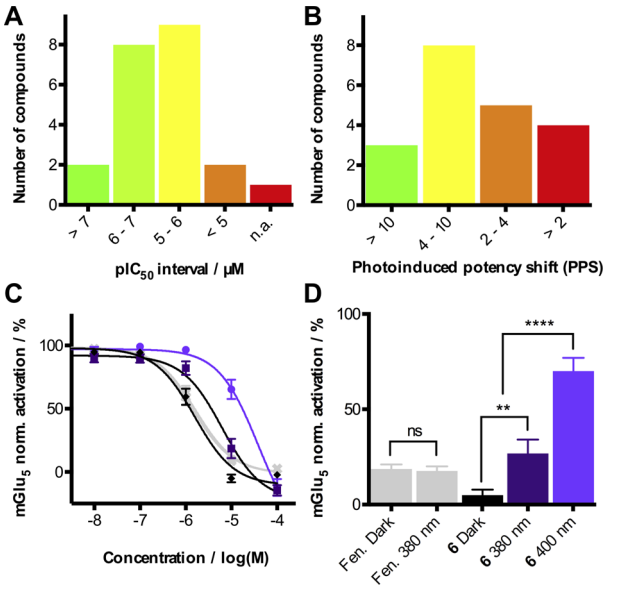

Figure 3. Pharmacological properties. (A) Distribution of compounds with the IC_{50} values obtained with an IP accumulation assay, with fenobam as the control. Approximately one-half of the compounds have potencies in the nanomolar range in dark conditions, and most of the compounds are more potent than fenobam (IC_{50} = 1.6 μM). (B) Distribution of compounds with the photoinduced potency shift (PPS) for the phenylazopyridines tested (see text). (C) IP accumulation dose–response curve of compound **6** with 100 nM of quisqualate in dark conditions (black), under illumination at 380 nm (dark violet), under illumination at 400 nm (bright violet). Gray curves correspond to the inverse agonist control (fenobam). (D) Percentage of activation of the $mGlu_5$ receptor with 10 μM **6** and 100 nM quisqualate. Analysis of variance (one-way ANOVA with Šidák correction for multiple comparisons; $^{**}p < 0.01$, $^{****}p < 0.0001$) showed significant differences between dark bar and 380 nm values, and also of 400 nm values with both dark and 380 nm values.

nanomolar IC_{50} (nearly 10- and 4-fold more potent than alloswitch-1 **1a**). Some other compounds were found to display potencies comparable to that of alloswitch-1, such as **1d** and **1g–k**, whereas **1b**, **1c**, **1l**, **3b**, **3c**, **4**, **5**, and **6** displayed micromolar IC_{50}, and some other even lower potencies (**3a**, **7**, and **8**). Singularly, compound **2**, a derivative of alloswitch-1 where the phenylazopyridine scaffold is replaced by an azobenzene, only partially inhibits the response of $mGlu_5$ (Supporting Information) despite its micromolar potency. A plausible explanation for this different behavior might be attributed to a different binding mode to the receptor, which would prevent the full antagonistic activity found for most of the phenylazopyridines. To investigate this point we performed a computational docking study for compounds **2**, **1e**, and **1f** in an $mGlu_5$ crystal structure.[33] The results obtained showed different binding modes for the azobenzene **2** compared to phenylazopyridines **1e** and **1f**, which resulted to be very similar to the docking previously reported for alloswitch-1 (**1a**).[34] These differences in the binding modes might affect $mGlu_5$ functionality despite not affecting considerably the binding energies, which are directly related to the affinity to $mGlu_5$ receptor (Supporting Information).

In these assays, the illumination at 380 nm induced a right shift of the dose–response curves when compared to the nonilluminated controls, compatible with a loss of the NAM potency of the *cis* isomers. Therefore, to quantify the effectiveness of the compound photoswitching, we introduced the term "photoinduced potency shift" (PPS) as the ratio of the IC_{50}s under illumination and in dark conditions. We obtained a wide variety of PPS (Table 1, Figure 2B), which are not correlated with the potency of each compound (Supporting Information), but have a significant correlation with the PIS (r = 0.77, $P < 0.0001$), extracted from the UV–vis absorption spectra (Figure 2A,B). This would indicate that the functional photoswitching of the receptor in living cells is similar to that observed in solution for the isolated compounds (Supporting Information).

We found very potent compounds with high PPS, such **1e** and **1f** (PPS (**1e**) = 3.7 and PPS (**1f**) = 4.8), but the higher value of PPS of compound **1f** defines it as a stronger candidate to control $mGlu_5$ activity with light. In addition, we could find interesting compounds with IC_{50}s in the micromolar range and very high PPS, such as **1b**, **3c**, or **6**. Specifically, compound **6** displayed large photoswitching capacities when it was illuminated at 400 nm (PPS = 12.3), much better than those observed at 380 nm (PPS = 4.4) (Figure 3C). Again, these results are consistent with the wavelength dependence observed in the *trans–cis* isomerization experiments of compound **6**. This effect was further quantified at a single 10 μM dose of **6** in the same cell-based assay (Figure 3D). In the dark, compound **6** induced a practically complete inhibition of $mGlu_5$, and under 380 nm light, it still induced a 75% inhibition. However, when 400 nm light was applied, the inhibition was reduced to 25%, compatible with the improved photoisomerization at this wavelength, as shown above. This particular experiment opens the possibility of inducing wavelength-dependent effects to fine-control the activity of the receptor with light, which in conventional pharmacology would require applying different concentrations of ligand.

Real-Time Photoswitching in Individual Cells. We next evaluated the possible application of the observed photoswitching to a reversible real-time control of $mGlu_5$ receptor. Hence, we selected the most representative phenylazopyridine compounds and tested their effects by time course of intracellular calcium in individual HEK293 cells overexpressing $mGlu_5$ receptor. In the dark, all tested compounds antagonized the calcium oscillations evoked by the activation of $mGlu_5$ with quisqualate, although the inhibition with **5** and **6** was not complete, in accordance with the low potency found in IP accumulation assays (Table 1, Supporting Information).

After a period in the dark, illumination with 380 nm light induced the photoisomerization of the phenylazopyridines and reestablished the calcium oscillations observed in response to the orthosteric agonist (Figures 4AB). This effect was reversed by green illumination and could be repeated over two light cycles for all compounds, demonstrating a reversible photoswitch in the cellular assays as well as a real-time control of the biological activity of $mGlu_5$ receptor with light (Figures 4AB). For some compounds we observed that, under 380 nm light, the frequency of calcium oscillations was increased compared to that observed with the orthosteric agonist alone (Figure 4B),

DOI: 10.1021/acscentsci.6b00353
ACS Cent. Sci. 2017, 3, 81–91

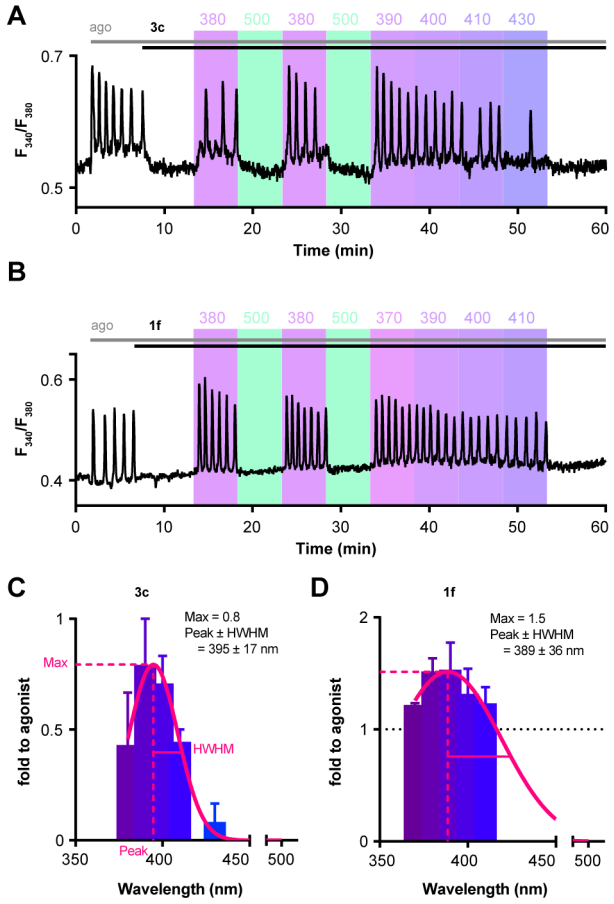

Figure 4. Calcium imaging in individual cells illustrates the light-dependency of $mGlu_5$ inhibition by compounds **1f** and **3c**. (A, B) Fluorescence ratio (F_{340}/F_{380}) over time of calcium indicator Fura-2 loaded in mGlu5-expressing HEK293 cells. Cells were challenged with an $mGlu_5$ agonist (ago, gray line, 3 μM quisqualate), 1 μM **3c** (A) or 1 μM **1f** (B) (black lines), and different illumination wavelengths (six, ranging between 370 and 500 nm) indicated by color boxes and corresponding numbers above. (C, D) Quantification of the light-induced receptor activity in the presence of **3c** (C) or **1f** (D) at indicated illumination wavelengths. Data are presented as mean ± SEM of the normalized calcium oscillation frequency. The frequency of calcium oscillations during an illumination period (5 min) was calculated as number of oscillations per minute, and normalized to the initial response to the agonist. Peak, half-width at half-maximum (HWHM), and maximum (Max) values were inferred by fitting the data shown in the graph to a Gaussian function (magenta curve).

suggesting an overactivation or an increased signaling of $mGlu_5$ receptors.

After violet–green light cycles, we additionally illuminated the cells with several wavelengths around 380 nm, to identify the best wavelength for restoring $mGlu_5$ activity (Figure 4AB). The oscillatory frequencies for each illumination period were normalized to the response to the agonist alone, plotted versus the wavelength used for illumination, and we fitted a Gaussian curve (Figures 4CD, Supporting Information). These results demonstrate that phenylazopyridines not only are able to switch *on* and *off* the $mGlu_5$ receptor upon green and violet illumination wavelengths but also can induce a fine-tuning of its activity. In addition, each compound of the series depends on different wavelengths for optimal photoswitching (peak), has broader or sharper "functional" absorption bands (HWHM), and presents varying degrees of receptor overactivation (Figure 5). For example, compound **1e**, which was found to be the most potent in the IP accumulation assay, is the most effective

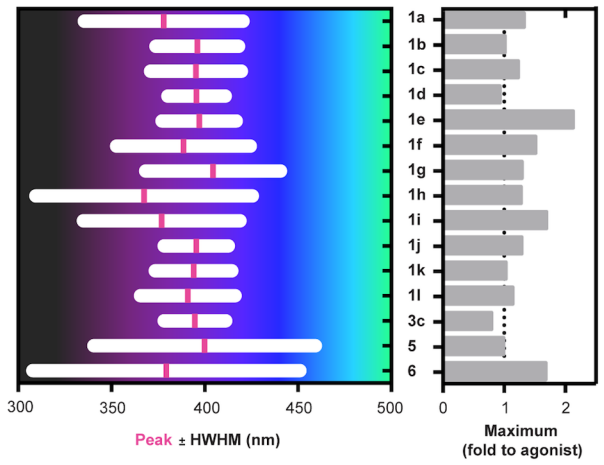

Figure 5. Summary of wavelength–activity relationships in single-cell experiments. In the left graph, magenta bars indicate the illumination wavelength (peak) at which the maximum light-induced receptor activity is obtained for the compounds indicated. White bars represent the range of wavelengths at which the light-induced activity is equal to half the maximum response or more (half-width at half-maximum, HWHM). The maximum amplitude of the light-induced receptor activity is reported in the graph on the right, and expressed as times the response to agonist of the naive receptors. These three parameters (peak, HWHM, and maximum) describe the Gaussian fitting performed for all compounds on the original data from single-cell experiments, as exemplified for **1f** and **3c** in Figure 4C,D. Original data were obtained from calcium imaging experiments in individual cells (done as described in Figure 4A,B).

in inducing an overactivation under violet illumination (>2-fold to agonist activation), whereas compound **3c** only recovered the response to quisqualate alone (Figure 5). The spectral range to achieve this activation also depends on the compound. Some have a narrow range, such as **1d** or **3c**, whereas others display a wider wavelength range, as **1h**, **5**, or **6**.

A related control of the frequency of $mGlu_5$ calcium oscillations was previously reported applying different concentrations of a conventional NAM[35] in different cell cultures. In contrast, the use of photoswitchable NAMs allows adjusting the effective ligand concentration by illuminating a single dose with specific wavelengths. This suggests a way to regulate the receptor response with a high spatiotemporal precision.

Zebrafish *in Vivo* Screening. We finally selected the active phenylazopyridines with a suitable efficacy in IP accumulation assays and tested on zebrafish larvae behavioral assays.

The activity of all compounds was first evaluated by monitoring zebrafish locomotion in dark conditions. Thus, after 10 μM administration of each compound in the swimming medium, we recorded the larva track during 30 min and the free-swimming distance of every animal was integrated at 5 min intervals (Figure 6B, Supporting Information). As a non-photoswitchable control, we used 2-BisPEB, which is a potent NAM of $mGlu_5$[36] because fenobam, previously used in cell-based assays, did not show significant differences with the vehicle. Otherwise, 2-BisPEB significantly inhibited the zebrafish motility, in line with the best phenylazopyridines of this series, such as **1a** and **1f** (Figure 6B).

In line with their $mGlu_5$ NAM activities, all the tested phenylazopyridines induced inhibition of the zebrafish motility

DOI: 10.1021/acscentsci.6b00353
ACS Cent. Sci. 2017, 3, 81–91

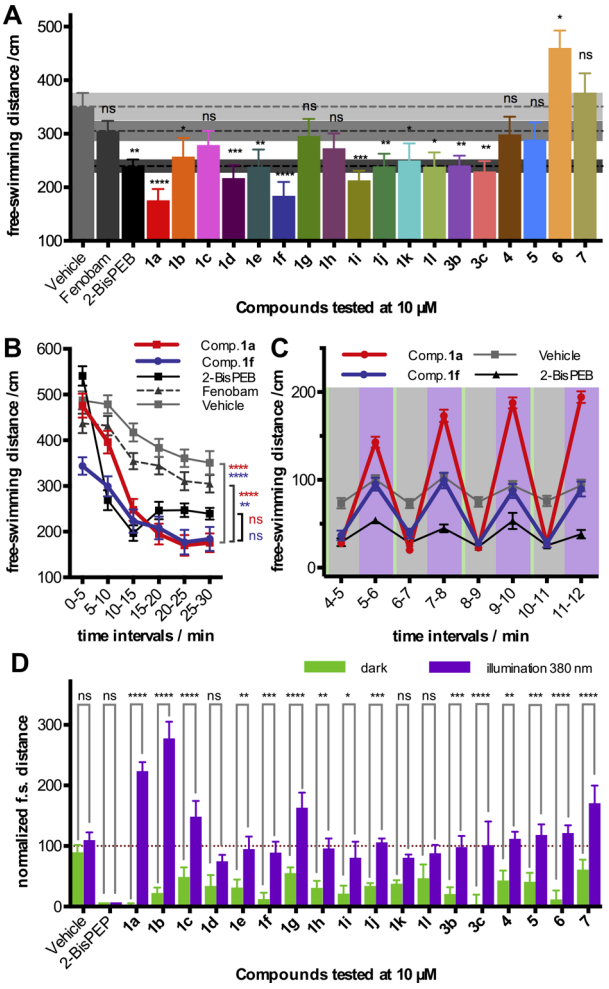

Figure 6. *In vivo* screening in 7-day-old zebrafish larvae. (A) Integration of free-swimming distances in the dark during 5 and 25 min after the administration of compounds **1a**–**l**, **2b**,**c** and **4**–**7** to afford a 10 μM concentration in the medium, extracted from individual plots (Supporting Information). Values correspond to the mean and the SEM of the behavior of 30 animals minimum. Analysis of variance showed statistically significant differences of the responses of some compounds with respect to vehicle. Values correspond to the mean and the SEM of the behavior of 30 animals minimum. (B) In the dark, compounds **1a** and **1f** decreased the motility of zebrafish 30 min after compound administration (10 μM) to an extent similar to that of 2-BisPEB. The free-swimming distances were integrated every 5 min during 30 min. Fenobam had a weak nonsignificant effect when compared to vehicle. Values correspond to the mean and the SEM of the behavior of 30 animals minimum. Analysis of variance (two-way (compound, time) ANOVA with time as repeated measure and including the Šidák correction for multiple testing; $*p < 0.05$, $**p < 0.01$, $***p < 0.001$, $****p < 0.0001$). (C) Effect of light/dark cycles. Compounds **1a** and **1f** at 10 μM inhibit animal motility similarly to 2-bisPEB in the dark (gray background), whereas under violet light (violet background) fish treated with **1f** recover a similar behavior to vehicle treated controls (blue line). Zebrafish larvae treated with **1a** experience an increase of their normal motility under violet light (red line). In the figure we show the light/dark cycles from 4 to 12 min. Values correspond to the mean and the SEM of the behavior of 24 animals minimum. (D) *In vivo* photoswitching efficacy of compounds **1a**–**l**, **2b**,**c**, and **4**–**7** with the corresponding variance analysis. Each bar corresponds to the mean of the sum of the free swimming distances in all the dark or violet illuminated points for each experiment (4 experiments with 6 animals per experiment) subtracting the corresponding sum of distances of the 2-BisPEB-treated animals and normalizing the distances by the lower distance mean of the set (0%) and the mean corresponding to the vehicle-treated animals (100%). The subtraction of the 2-BisPEB effect was done to minimize the effect of the light not corresponding to the effect of the administered compounds. The error bars correspond to the associated SEM. Analysis of variance (two-way (compound, light conditions) ANOVA with light conditions as a repeated measure and including the Šidák correction for multiple comparisons; $*p < 0.05$, $**p < 0.01$, $***p < 0.001$, $****p < 0.0001$).

25 min after their administration with different extents, except compounds **6** and **7**, which induced a slight increase in the animal motility (Figure 6A) when comparing to the vehicle treated animals. In contrast, compounds **1e**, **1g**, and **1h**, which display nanomolar potency in IP accumulation assays, inhibited zebrafish motility with a lower efficacy than expected. The reasons for these deviations are presently unknown and can be related to the multiple factors influencing the *in vivo* activity and the characteristics of the assay. Remarkably, the magnitude of the inhibition of the animal motility for most of the compounds was comparable to the potencies in cell-based assays (Supporting Information).

To evaluate the photoswitching effects *in vivo* we performed an extension of the assay with the same animals right after the experiments done in dark conditions. We applied six repetitive light cycles consisting of 1 min in dark conditions and 1 min under violet illumination (λ = 380 nm), and the animal motility was tracked with an integration of the free-swimming distance every 60 s cycle. Between the violet illumination and the dark conditions, the fish were also illuminated during 5 s with white light to accelerate the phenylazopyridine relaxation from *cis* to *trans* configuration. Violet light prompted an increment of the motility respective to the dark conditions for all the zebrafish tested, including vehicle and 2-BisPEB-treated ones. However, 2-BisPEB-treated animals displayed a sustained inhibition of their motility compared to the vehicle treated animals independently of the light conditions (Figure 6C, Supporting Information).

As a general trend, all phenylazopyridines showed inhibitory effects in dark conditions that disappeared after shining 380 nm light, and it was recovered in the following dark cycle, defining a fully reversible process (Supporting Information). In addition, we found two different behaviors under 380 nm illumination that are dependent on the compound used: (a) a motility in line with vehicle-treated larvae or (b) an overactivation of the animal motility, which exceeded the levels displayed by vehicle-treated larvae. Compounds **1a** and **1f** constitute a prototypical example of these behavioral modes (Figure 6C), while in dark conditions they equally inhibit the animal motility with a high efficacy.

This *in vivo* overactivation after applying violet illumination could be related to the overactivation observed in real-time cell-based assays and was evident for compounds **1b**, **1c**, **1g**, and **7**, or for compounds **4**, **5**, and **6**, as a milder effect (Figure 6D, Supporting Information). All these phenylazopyridine derivatives comprise a set of compounds with very different potencies, from low nanomolar ranges to micromolar IC_{50}s in IP accumulation assays, and structurally have three aromatic rings with a phenyl group at the amide end. In contrast, either the group of compounds that did not prompt this over-activation does not have this third aromatic ring or, if it is

DOI: 10.1021/acscentsci.6b00353
ACS Cent. Sci. 2017, 3, 81–91

present, its electron density is low due to the presence of electron-withdrawing groups, like fluorine, or they have pyridines, which are intrinsically electron poor. Compound 7 constitutes a particular case, since it also induces overactivation under illumination and includes a 2-pyridylcarboxamide ring as the third aromatic ring. However, it is the only compound tested with 1,3 substitution in the central ring, which is expected to induce a lower influence on the π electron density of the azo bond. Intriguingly, not all the compounds that induce this overactivation do it in real-time cell assays. For example, compounds **1e**, **1f**, and **1i**, with a higher overactivation effect in cell-based assays, did not induce a measurable overactivation in animal motility. In contrast, **1b**, unable to produce the receptor overactivations in cell-based assays, induced the highest overactivation *in vivo*. This may be due to differences in these two assays, which use different illumination protocols and test mammalian and zebrafish $mGlu_5$ receptors respectively, whose functionalities can differ considerably. In any case, this atypical effect appears to be light dependent, could only be detected with photoswitchable compounds, and will be subject of future studies.

Regarding the *in vivo* photoswitchable properties of the phenylazopyridines, all of them induce photoswitching in zebrafish motility (Figure 6D) to different extents. The compounds that promoted an overactivation of the animal motility under violet light show higher statistical significances in their photoswitching. Even so, differences for the rest of compounds were still significant, except for compound **1d**, whose *in vivo* activity was abnormally weak, and **1k** and **1l**, which also performed poorly in cell assays (PPS(**1k**) = 1.3, PPS(**1l**) = 1.2), probably as a consequence of their limited intrinsic low photoisomerization capacity (PIS_{380}(**1k**) = 1, PIS_{500}(**1k**) = 1; PIS_{380}(**1l**) = 1 PIS_{500}(**1l**) = 0). In fact, if compound **1d** and the compounds with overactivation behavior are not taken into account, the difference between the violet and dark values of each compound in Figure 6D correlates with photoisomerization score (PIS) (r = 0.70, P = 0.025) and with photoinduced potency shift (PPS) logarithm (r = 0.83, P = 0.0031) (Supporting Information), showing a remarkable consistency of the photoisomerization throughout the different assays, from compound in solution to cell-based *in vitro* assays and *in vivo* behavioral experiments.

Rodent *in Vivo* Pain Assay. Next, we aimed to assess photoswitching in rodent tissue. We used a classical animal model of pain based on the intraplantar administration of formalin (Supporting Information) since local plantar blockade of group I mGluRs was reported to reduce the spontaneous formalin behavior.[37] Thus, we monitored the local efficacy of compounds **1e** and **1f** to modify the formalin-mediated nociception in dark and upon illumination with violet light (Figure 7A). As expected, both compounds showed anti-nociceptive properties in dark conditions since the mouse licking paw time was significantly reduced when compared to the vehicle condition (Figure 7A).

Interestingly, compounds **1f** and **1e** were equipotent or even more effective, respectively, when compared to the $mGlu_5$ NAM reference compound used (raseglurant, Chart 1, Figure 7A). Importantly, the intrinsic antinociceptive efficacy of both compounds was significantly reduced upon external paw illumination with violet light, thus suggesting that local photoisomerization was achieved while monitoring nociception (Figure 7A).

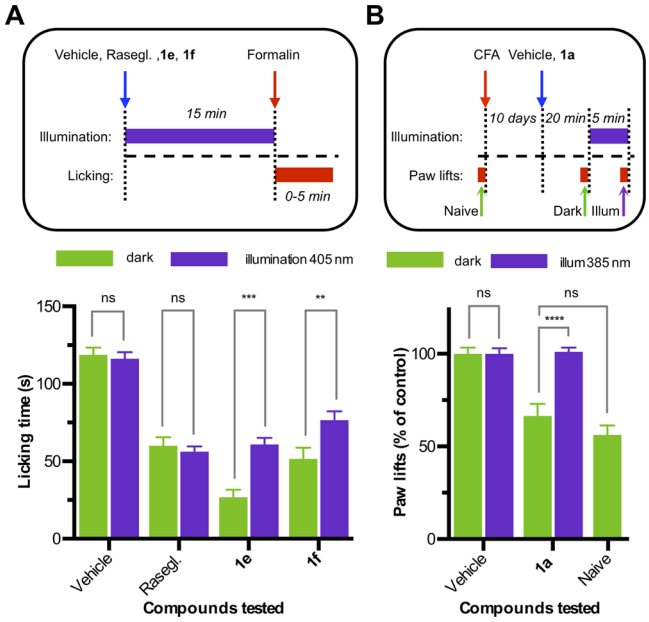

Figure 7. Photoswitching of pain-like behavior in mice. (A) Local photoswitching in the mouse hindpaw. The mouse hindpaw was injected with vehicle (20% DMSO + 20% Tween-80 in saline), 5 mM raseglurant (Rasegl.), 5 mM compound **1e** or 5 mM compound **1f** and then illumination at 405 nm (or dark) during 15 min was performed (n = 6 for each condition). Subsequently, the total hindpaw licking (in seconds) was measured during 5 min after the intraplantar injection of formalin solution (2.5% paraformaldehyde). The scheme of the protocol used is depicted in the upper inset. Analysis of variance (one-way ANOVA with Šidák correction for multiple comparisons; $^{**}p < 0.01$, $^{***}p < 0.001$) showed significant differences between dark and 405 nm values for phenylazopyridines **1e** and **1f**, but not for vehicle and raseglurant. (B) Local photoswitching in mouse amygdala. Persistent inflammatory pain was induced by unilateral intraplantar injection of 30 μL of complete Freund's adjuvant (CFA) in the left hind paw. Mechanical allodynia was measured by stimulating the CFA-treated hindpaw with a 1.4 g von Frey filament after intra-amygdala injection of vehicle (0.003% DMSO in PBS, n = 11) or compound **1a** (300 nM, n = 13) in dark condition and with amygdala illumination at 385 nm. Naive-mouse mechanical sensitivity was measured before CFA injection (n = 11). The scheme of the protocol used is also depicted in the upper inset. Analysis of variance (one-way ANOVA with Šidák correction for multiple comparisons; $^{****}p < 0.0001$) showed significant differences between dark and 385 nm values for **1a** but not for vehicle and showed nonsignificant differences between the naive mice and those treated with **1a** with no illumination.

We next examined the *in vivo* phenylazopyridine photoswitching in mouse CNS, since $mGlu_5$ receptor is expressed in amygdala and its activation is related to pain-like effects.[38] We evaluated the mechanical allodynia in a CFA-induced persistent inflammatory pain model by using the von Frey technique (Supporting Information). Mice were stereotaxically implanted with hybrid optic and fluid cannulas in the amygdala allowing the controlled administration of compounds and light in freely behaving animals. Amygdala injection of alloswitch-1 (**1a**) restored the mechanical sensitivity to the level of naive mice (before inflammation), compatible with the *trans* active form of the compound (Figure 7B). The observed analgesic effect was abolished after amygdala illumination at 385 nm (Figure 7B). That suggests that the local photoisomerization of **1a** from *trans* to *cis* configuration in the amygdala can control the analgesic effect of the compound in peripheral tissues. In

DOI: 10.1021/acscentsci.6b00353
ACS Cent. Sci. 2017, 3, 81−91

contrast, 385 nm illumination induced no effect with vehicle conditions (Figure 7B).

These results confirm that phenylazopyridines can be used for local control of $mGlu_5$ with light in behaving rodents, both peripherally and in the CNS, opening uses of photopharmacology in disease models and behavioral assays.

CONCLUDING REMARKS

We synthesized a series of photoswitchable $mGlu_5$ NAMs based on the phenylazopyridine scaffold, with a robust SAR, since almost all the *trans* isomers were active on $mGlu_5$ and half of them significantly inhibited zebrafish motility at 10 μM concentration. We obtained compounds with different photoisomerization properties, and their translation to *in vitro* and *in vivo* assays was also robust, since very few compounds lost their photoswitching properties in any of the different subsequent assays in spite of the increasing complexity of the biological tests. From these compounds, we obtained excellent photoswitching behavior in all the assays performed with compounds **1a**, **1f**, **1i**, **1j**, and **3c** as well as **6**, in which we afforded a more powerful effect at more cell-compatible blue-shifted wavelengths. To account for the efficiency in the photoswitching we have proposed two parameters: the photoisomerization score (PIS) and the photoinduced potency shift (PPS).

Additionally, these phenylazopyridines allowed us to define a way to perform a fine control of $mGlu_5$ receptor activity by tuning the wavelength of illumination between 360 and 500 nm, and, depending on the compound used, we were able to control an overactivation of the receptor. This functional overactivation was also detected *in vivo* after treating zebrafish larvae with some specific compounds, but not with others. The reasons for this light-dependent atypical effect could be linked to the potentiation of calcium responses in single cell assays and require further investigation. Finally, $mGlu_5$ NAM phenylazopyridines showed analgesic effects in rodents, which can be regulated by peripheral violet illumination or directly in the CNS, thus validating the potential usefulness of allosteric $mGlu_5$ photopharmacology *in vivo*. Overall, photoswitchable phenylazopyridines reveal new paradigms on the ligand-induced protein responses with potential to add a new modulatory dimension to drug therapeutics.

ASSOCIATED CONTENT

Supporting Information

The Supporting Information is available free of charge on the ACS Publications website at DOI: 10.1021/acscentsci.6b00353.

Experimental details, chemical and photo- and biochemical characterization of **1**−**9**, and computational details (PDF)

AUTHOR INFORMATION

Corresponding Authors

*E-mail: pau@icrea.cat.

*E-mail: amadeu.llebaria@iqac.csic.es.

ORCID

Amadeu Llebaria: 0000-0002-8200-4827

Present Address

[‖]X.G.-S.: Division of Medicinal Chemistry, VU University Amsterdam, De Boelelaan 1108, 1081 HV Amsterdam, The Netherlands.

Notes

The authors declare no competing financial interest.

ACKNOWLEDGMENTS

We are grateful to C. Serra and L. Muñoz for synthetic and analytical support, F. Malhaire for technical support in cell-based pharmacological assays, and Y. Pérez for NMR support. This research has been supported by RecerCaixa foundation (2010ACUP00378 to P.G., J.G., and A.L.), the Marató de TV3 Foundation (110230 to J.G., 110231 to A.L., 110232 to C.G., and 111531 to P.G.), the Catalan government (2010 BP-A 00194 to X.R., 2012FI_B 01122 to S.P., 2012 CTP 00033 and 2012 BE1 00597 to X.G.-S., 2014SGR-1251 to P.G., and 2014SGR-00109 to A.L.), the Spanish Government (CTQ2014-57020-R and PCIN-2013-017-C03-01 to A.L., PIE14/00034, SAF2014-55700-P, and PCIN-2013-019-C03-03 to F.C., and SAF2014-58396-R to J.G.), AWT (SBO-140028) to F.C., and the ERANET Neuron LIGHTPAIN project (to A.L., F.C., J.G., and J.-P.P.); SynBio MODULIGHTOR, Human Brain Project WAVESCALES and Ramon Areces foundation grants (to P.G.); the Agence Nationale de la Recherche (ANR-16-CE16-0010 to A.L. and C.G.).

ABBREVIATIONS

GPCR, G protein-coupled receptor; $mGlu_5$, metabotropic glutamate receptor subtype 5; NAM, negative allosteric modulator; HPLC-PDA-MS, high performance liquid chromatography coupled to photodiode array detector and a mass spectrometer; UV−vis, ultraviolet−visible; HEK293, human embryonic kidney 293; IP, myo-inositol phosphate; ANOVA, analysis of variance; SAR, structure−activity relationship; CNS, central nervous system; CFA, complete Freund's adjuvant

REFERENCES

(1) Drews, J. Drug discovery: a historical perspective. *Science* **2000**, *287*, 1960−1964.

(2) Hay, M.; Thomas, D. W.; Craighead, J. L.; Economides, C.; Rosenthal, J. Clinical development success rates for investigational drugs. *Nat. Biotechnol.* **2014**, *32*, 40−51.

(3) Paul, S. M.; Mytelka, D. S.; Dunwiddie, C. T.; Persinger, C. C.; Munos, B. H.; Lindborg, S. R.; Schacht, A. L. How to improve R&D productivity: the pharmaceutical industry's grand challenge. *Nat. Rev. Drug Discovery* **2010**, *9*, 203−214.

(4) Kramer, R. H.; Mourot, A.; Adesnik, H. Optogenetic pharmacology for control of native neuronal signaling proteins. *Nat. Neurosci.* **2013**, *16*, 816−823.

(5) Velema, W. A.; Szymanski, W.; Feringa, B. L. Photopharmacology: beyond proof of principle. *J. Am. Chem. Soc.* **2014**, *136*, 2178−2191.

(6) Gorostiza, P.; Isacoff, E. Y. Optical switches for remote and noninvasive control of cell signaling. *Science* **2008**, *322*, 395−399.

(7) Nevola, L.; Martin-Quiros, A.; Eckelt, K.; Camarero, N.; Tosi, S.; Llobet, A.; Giralt, E.; Gorostiza, P. Light-regulated stapled peptides to inhibit protein-protein interactions involved in clathrin-mediated endocytosis. *Angew. Chem., Int. Ed.* **2013**, *52*, 7704−7708.

(8) Broichhagen, J.; Trauner, D. The in vivo chemistry of photoswitched tethered ligands. *Curr. Opin. Chem. Biol.* **2014**, *21*, 121−127.

(9) Schoenberger, M.; Damijonaitis, A.; Zhang, Z.; Nagel, D.; Trauner, D. Development of a new photochromic ion channel blocker via azologization of fomocaine. *ACS Chem. Neurosci.* **2014**, *5*, 514−518.

(10) Broichhagen, J.; Frank, J. A.; Trauner, D. A roadmap to success in photopharmacology. *Acc. Chem. Res.* **2015**, *48*, 1947−1960.

DOI: 10.1021/acscentsci.6b00353
ACS Cent. Sci. 2017, 3, 81−91

(11) Pittolo, S.; Gomez-Santacana, X.; Eckelt, K.; Rovira, X.; Dalton, J.; Goudet, C.; Pin, J. P.; Llobet, A.; Giraldo, J.; Llebaria, A.; Gorostiza, P. An allosteric modulator to control endogenous G protein-coupled receptors with light. *Nat. Chem. Biol.* **2014**, *10*, 813−815.
(12) Bartels, E.; Wassermann, N. H.; Erlanger, B. F. Photochromic activators of the acetylcholine receptor. *Proc. Natl. Acad. Sci. U. S. A.* **1971**, *68*, 1820−1823.
(13) Volgraf, M.; Gorostiza, P.; Szobota, S.; Helix, M. R.; Isacoff, E. Y.; Trauner, D. Reversibly caged glutamate: a photochromic agonist of ionotropic glutamate receptors. *J. Am. Chem. Soc.* **2007**, *129*, 260−261.
(14) Stein, M.; Middendorp, S. J.; Carta, V.; Pejo, E.; Raines, D. E.; Forman, S. A.; Sigel, E.; Trauner, D. Azo-propofols: photochromic potentiators of GABA(A) receptors. *Angew. Chem., Int. Ed.* **2012**, *51*, 10500−10504.
(15) Broichhagen, J.; Jurastow, I.; Iwan, K.; Kummer, W.; Trauner, D. Optical control of acetylcholinesterase with a tacrine switch. *Angew. Chem., Int. Ed.* **2014**, *53*, 7657−7660.
(16) Broichhagen, J.; Schonberger, M.; Cork, S. C.; Frank, J. A.; Marchetti, P.; Bugliani, M.; Shapiro, A. M.; Trapp, S.; Rutter, G. A.; Hodson, D. J.; Trauner, D. Optical control of insulin release using a photoswitchable sulfonylurea. *Nat. Commun.* **2014**, *5*, 5116.
(17) Borowiak, M.; Nahaboo, W.; Reynders, M.; Nekolla, K.; Jalinot, P.; Hasserodt, J.; Rehberg, M.; Delattre, M.; Zahler, S.; Vollmar, A.; Trauner, D.; Thorn-Seshold, O. Photoswitchable Inhibitors of Microtubule Dynamics Optically Control Mitosis and Cell Death. *Cell* **2015**, *162*, 403−411.
(18) Krop, S. The local anesthetic action of beta-phenylazo alpha-alpha'diamino pyridine monohydrochloride (pyridium) and its metabolites. *Curr. Res. Anesth. Analg.* **1946**, *25*, 110−114.
(19) Sierecki, E.; Sinko, W.; McCammon, J. A.; Newton, A. C. Discovery of small molecule inhibitors of the PH domain leucine-rich repeat protein phosphatase (PHLPP) by chemical and virtual screening. *J. Med. Chem.* **2010**, *53*, 6899−6911.
(20) Kim, Y. C.; Brown, S. G.; Harden, T. K.; Boyer, J. L.; Dubyak, G.; King, B. F.; Burnstock, G.; Jacobson, K. A. Structure-activity relationships of pyridoxal phosphate derivatives as potent and selective antagonists of P2 × 1 receptors. *J. Med. Chem.* **2001**, *44*, 340−349.
(21) Zhang, G.; Plotnikov, A. N.; Rusinova, E.; Shen, T.; Morohashi, K.; Joshua, J.; Zeng, L.; Mujtaba, S.; Ohlmeyer, M.; Zhou, M. M. Structure-guided design of potent diazobenzene inhibitors for the BET bromodomains. *J. Med. Chem.* **2013**, *56*, 9251−9264.
(22) Geldenhuys, W. J.; Ko, K. S.; Stinnett, H.; Van der Schyf, C. J.; Lim, M. H. Identification of multifunctional small molecule-based reversible monoamine oxidase inhibitors. *MedChemComm* **2011**, *2*, 1099−1103.
(23) Mitra, K.; Patil, S.; Kondaiah, P.; Chakravarty, A. R. 2-(Phenylazo)pyridineplatinum(II) catecholates showing photocytotoxicity, nuclear uptake, and glutathione-triggered ligand release. *Inorg. Chem.* **2015**, *54*, 253−264.
(24) Chakraborty, I.; Carrington, S. J.; Mascharak, P. K. Photodelivery of CO by designed PhotoCORMs: correlation between absorption in the visible region and metal-CO bond labilization in carbonyl complexes. *ChemMedChem* **2014**, *9*, 1266−1274.
(25) Conn, P. J. Physiological roles and therapeutic potential of metabotropic glutamate receptors. *Ann. N. Y. Acad. Sci.* **2003**, *1003*, 12−21.
(26) Varney, M. A.; Cosford, N. D.; Jachec, C.; Rao, S. P.; Sacaan, A.; Lin, F. F.; Bleicher, L.; Santori, E. M.; Flor, P. J.; Allgeier, H.; Gasparini, F.; Kuhn, R.; Hess, S. D.; Velicelebi, G.; Johnson, E. C. SIB-1757 and SIB-1893: selective, noncompetitive antagonists of metabotropic glutamate receptor type 5. *J. Pharmacol. Exp. Ther.* **1999**, *290*, 170−181.
(27) Gómez-Santacana, X.; Rovira, X.; Dalton, J. A.; Goudet, C.; Pin, J. P.; Gorostiza, P.; Giraldo, J.; Llebaria, A. A double effect molecular switch leads to a novel potent negative allosteric modulator of metabotropic glutamate receptor 5. *MedChemComm* **2014**, *5*, 1548−1554.
(28) Emmitte, K. A. mGlu5 negative allosteric modulators: a patent review (2010−2012). *Expert Opin. Ther. Pat.* **2013**, *23*, 393−408.
(29) García-Amorós, J.; Velasco, D. Recent advances towards azobenzene-based light-driven real-time information-transmitting materials. *Beilstein J. Org. Chem.* **2012**, *8*, 1003−1017.
(30) Garcia-Amoros, J.; Nonell, S.; Velasco, D. Light-controlled real time information transmitting systems based on nanosecond thermally-isomerising amino-azopyridinium salts. *Chem. Commun.* **2012**, *48*, 3421−3423.
(31) Asano, T.; Okada, T. Thermal Z−E isomerization of azobenzenes. The pressure, solvent, and substituent effects. *J. Org. Chem.* **1984**, *49*, 4387−4391.
(32) Bandara, H. M. D.; Burdette, S. C. Photoisomerization in different classes of azobenzene. *Chem. Soc. Rev.* **2012**, *41*, 1809−1825.
(33) Dore, A. S.; Okrasa, K.; Patel, J. C.; Serrano-Vega, M.; Bennett, K.; Cooke, R. M.; Errey, J. C.; Jazayeri, A.; Khan, S.; Tehan, B.; Weir, M.; Wiggin, G. R.; Marshall, F. H. Structure of class C GPCR metabotropic glutamate receptor 5 transmembrane domain. *Nature* **2014**, *511*, 557−562.
(34) Dalton, J. A.; Lans, I.; Rovira, X.; Malhaire, F.; Gomez-Santacana, X.; Pittolo, S.; Gorostiza, P.; Llebaria, A.; Goudet, C.; Pin, J. P.; Giraldo, J. Shining Light on an mGlu5 Photoswitchable NAM: A Theoretical Perspective. *Curr. Neuropharmacol.* **2016**, *14*, 441−454.
(35) Nash, M. S.; Schell, M. J.; Atkinson, P. J.; Johnston, N. R.; Nahorski, S. R.; Challiss, R. A. Determinants of metabotropic glutamate receptor-5-mediated Ca2+ and inositol 1,4,5-trisphosphate oscillation frequency. Receptor density versus agonist concentration. *J. Biol. Chem.* **2002**, *277*, 35947−35960.
(36) Molck, C.; Harpsoe, K.; Gloriam, D. E.; Clausen, R. P.; Madsen, U.; Pedersen, L. O.; Jimenez, H. N.; Nielsen, S. M.; Mathiesen, J. M.; Brauner-Osborne, H. Pharmacological characterization and modeling of the binding sites of novel 1,3-bis(pyridinylethynyl)benzenes as metabotropic glutamate receptor 5-selective negative allosteric modulators. *Mol. Pharmacol.* **2012**, *82*, 929−937.
(37) Bhave, G.; Karim, F.; Carlton, S. M.; Gereau, R. W. Peripheral group I metabotropic glutamate receptors modulate nociception in mice. *Nat. Neurosci.* **2001**, *4*, 417−423.
(38) Kolber, B. J.; Montana, M. C.; Carrasquillo, Y.; Xu, J.; Heinemann, S. F.; Muglia, L. J.; Gereau, R. W. Activation of metabotropic glutamate receptor 5 in the amygdala modulates pain-like behavior. *J. Neurosci.* **2010**, *30*, 8203−8213.

DOI: 10.1021/acscentsci.6b00353
ACS Cent. Sci. 2017, 3, 81−91